NRC Research Press

ARTICLE

Acinetobacter baylyi long-term stationary-phase protein StiP is a protease required for normal cell morphology and resistance to tellurite

Blake Reichert, Amber J. Dornbusch, Joshua Arguello, Sarah E. Stanley, Kristine M. Lang, C. Phoebe Lostroh, and Margaret A. Daugherty

Abstract: We investigated the *Acinetobacter baylyi* gene *ACIAD1960*, known from previous work to be expressed during long-term stationary phase. The protein encoded by this gene had been annotated as a Conserved Hypothetical Protein, surrounded by putative tellurite resistance ("Ter") proteins. Sequence analysis suggested that the protein belongs to the DUF1796 putative papain-like protease family. Here, we show that the purified protein, subsequently named StiP, has cysteine protease activity. Deletion of *stiP* causes hypersensitivity to tellurite, altered population dynamics during long-term batch culture, and most strikingly, dramatic alteration of normal cell morphology. StiP and associated Ter proteins (the StiP–Ter cluster) are therefore important for regulating cell morphology, likely in response to oxidative damage or depletion of intracellular thiol pools, triggered artificially by tellurite exposure. Our finding has broad significance because while tellurite is an extremely rare compound in nature, oxidative damage, the need to maintain a particular balance of intracellular thiols, and the need to regulate cell morphology are ubiquitous.

Key words: long-term stationary phase, tellurite resistance, DUF1796, Ter domain, cell division.

Résumé : Nous avons fait l'étude du gène *ACIAD1960* d'*Acinetobacter baylyi*, qui selon des travaux antérieurs serait exprimé au cours de la phase stationnaire prolongée. La protéine codée par ce gène a été libellée « protéine hypothétique conservée » et est entourée de protéines putatives de résistance à la tellurite (« Ter »). Une analyse de la séquence a indiqué que la protéine appartiendrait à la famille hypothétique DUF1796 regroupant des protéases semblables à la papaïne. Nous démontrons dans cet ouvrage que la protéine purifiée, baptisée StiP, fait preuve d'une activité cystéine protéase. La délétion de *stiP* entraîne une hypersensibilité à la tellurite, des changements dans les dynamiques de populations lors de cultures prolongées en lots, et un changement manifeste et profond de la morphologie cellulaire normale. StiP et les protéines Ter associées (le groupe StiP–Ter) sont donc importantes dans la régulation de la morphologie cellulaire, et répondent vraisemblablement au dommage oxydatif et à l'épuisement des réserves intracellulaires de thiols qui seraient provoqués artificiellement par une exposition à la tellurite. Notre constatation a un impact d'envergure, car étant entendu que la tellurite est une substance extrêmement rare dans la nature, il en est tout autrement du caractère universel du dommage oxydatif et du besoin de maintenir un certain équilibre de thiols intracellulaires et de réguler la morphologie cellulaire. [Traduit par la Rédaction]

Mots-clés : phase stationnaire prolongée, résistance à la tellurite, DUF1796, domaine Ter, division cellulaire.

Introduction

Acinetobacter species are ubiquitous soil organisms that encounter competition for catabolic substrates in nature. *Acinetobacter baylyi* ADP1 was originally isolated from a strain termed BD4, which was isolated from soil using minimal medium with an unusual catabolic substrate, *meso*-2,3-butanediol, as the sole carbon source (Barbe et al. 2004; Taylor and Juni 1961*a*, 1961*b*). Like other *Acinetobacter* spp., strain ADP1 exhibits catabolic versatility, able to use diverse substrates such as alkanesulfonates, *p*-hydroxybenzoate, catechol, and salicylate esters, to name a few (Barbe et al. 2004). These characteristics suggest that the genus excels in its ability to oxidize diverse resources in the face of intense competition.

Starvation during long-term stationary phase (LTSP) can serve as a laboratory model for these natural competitive conditions, which bacteria are thought to experience in natural settings such as soils (Finkel 2006). This model has been used primarily to study *Escherichia coli*, though in previous work we discovered that *A. baylyi* cells can also be studied during LTSP. An initially clonal population of bacteria incubated in batch culture for weeks experiences 5 growth stages: the familiar lag, exponential, and (immediate) stationary phases, followed by death phase and LTSP. For clarity's sake, we refer to the phase that immediately follows exponential growth as "immediate stationary phase", and to the final stage of life in batch culture as "long-term stationary phase".

Prior to LTSP, most of the cells die, releasing cellular contents including DNA (Finkel and Kolter 2001; Zambrano et al. 1993).

Received 30 July 2013. Revision received 8 September 2013. Accepted 9 September 2013.

B. Reichert and M.A. Daugherty. Department of Chemistry and Biochemistry, Colorado College, 14 East Cache La Poudre Avenue, Colorado Springs, CO 80903, USA.
A.J. Dornbusch,* J. Arguello, S.E. Stanley, and C.P. Lostroh. Department of Biology, Colorado College, 14 East Cache La Poudre Avenue, Colorado Springs, CO 80903, USA.
K.M. Lang. Department of Physics, Colorado College, 14 East Cache La Poudre Avenue, Colorado Springs, CO 80903, USA.
Corresponding author: Margaret A. Daugherty (e-mail: MDaugherty@ColoradoCollege.edu).
*Present address: Department of Immunology, The Mayo Clinic, Rochester, MN 55902, USA.

Dead cells serve as a source of nutrition for starving survivors, which continue to reproduce despite the fierce competition for increasingly limited resources. Starving populations in LTSP are highly dynamic. Firstly, for each newly dead cell, slightly less than one new cell is "born" (reviewed in Finkel 2006). Secondly, cells in LTSP have a mutation rate approaching 1 mutation in 600 bp, much higher than that of cells during exponential phase (Finkel 2006). In fact, the initially clonal population of cells becomes genetically heterogeneous, and mutants that have beneficial traits arise and take over the population, until another more fit mutant arises, in a cyclical process that requires mutagenic DNA replication and repair processes (reviewed in Zinser and Kolter 1999, 2000, 2004; Zinser et al. 2003).

Other physiological changes that take place during LTSP have been described. For example, *E. coli*, *Geobacter sulfurreducens*, and *A. baylyi* cells become smaller and more spherical (Helmus et al. 2012; Lostroh and Voyles 2010; Zambrano et al. 1993). These changes suggest alterations in the synthesis of cell envelope components and in the regulation of the initiation of chromosome synthesis. Genes expressed during LTSP also indicate physiological traits such as use of DNA as a catabolic substrate, at least in *E. coli*. Their consumption of DNA requires proteins that are homologous to competence genes found in naturally competent organisms such as *A. baylyi* (Finkel and Kolter 2001).

In previous work, we examined *A. baylyi* cells during LTSP and identified 30 *lacZ* reporter fusions that are highly induced during LTSP compared with very low expression during exponential growth (Lostroh and Voyles 2010). The 30 induced genes include ones encoding anabolic and catabolic enzymes, gene expression proteins, DNA repair and competence proteins, stress response proteins, envelope proteins, and conserved hypothetical proteins. We became particularly interested in one of the conserved hypothetical proteins, ACIAD1960, because its coding sequence is surrounded by a group of enigmatic "tellurite resistance genes." Tellurite resistance has long been observed in some isolates of pathogenic bacteria, but the phenotype is puzzling because tellurite is extremely rare, while tellurite resistance and "Ter" proteins required for that resistance are widespread (Chasteen et al. 2009). The finding that ACIAD1960 is expressed during LTSP suggested to us that Ter proteins might have a role to play during starvation or other stressors, such as oxygen radicals or DNA damage, which are both encountered during LTSP and are also common in natural environments.

The focus of this work is therefore to ascertain whether *ACIAD1960* encodes an actual protein (rather than a hypothetical one) and to make progress discovering physiological activities associated with it. Toward that end, we used sequence analysis to examine the evolutionary history, genomic context, predicted domains, and predicted phenotypes of *ACIAD1960*. Next, we cloned *ACIAD1960* in an *E. coli* expression vector and purified the protein, and subsequently examined whether it has the cysteine protease activity predicted by a DUF1796 annotation. Finally, we tested the phenotypes predicted to be associated with deletion of the *ACIAD1960* gene and of surrounding "tellurite resistance" genes. Our results prompt removing *ACIAD1960* and its homologs from the realm of "hypothetical", and establish that DUF1796 proteins have cysteine protease activity. We name the *A. baylyi* protein StiP to reflect its discovery as a long-term *s*tationary-phase *i*nduced protein and its biochemical *p*rotease activity. Through study of a strain lacking *stiP*, we have also uncovered a novel link between so-called tellurite resistance proteins and regulation of cell division, which could be of broad significance.

Materials and methods

Culture conditions

Acinetobacter baylyi was obtained from the American Type Culture Collection (ATCC 33305; Manassas, Virginia, USA). Insertion–deletion mutants were obtained from Genoscope (de Berardinis et al. 2008). ADP1 was routinely maintained on Minimal Davis Agar (Sigma-Aldrich, St. Louis, Missouri, USA) with 10 mmol/L succinate (Thermo Fisher Scientific, Waltham, Massachusetts, USA). Mutants were maintained on Luria–Bertani (LB) (10 g tryptone (Beckton, Dickinson, and Company, Franklin Lakes, New Jersey, USA), 5 g yeast extract (Beckton, Dickinson), 10 g NaCl/L agar (Thermo Fisher Scientific)) containing 10 μg/mL kanamycin (Thermo Fisher Scientific). Cells were grown at 37 °C, with high aeration for all broths.

Sequence analysis

For sequence analysis, we used the Kyoto Enzymes, Genes, and Genomes database (KEGG), which provides tools to discover orthologs in other organisms (proteins with statistically significant similarity to the query, encoded by any of the other complete genomes in the database; www.genome.jp (Kanehisa and Goto 2000; Kanehisa et al. 2012)). To find domain predictions, we used the KEGG Motif tool and the National Center for Biotechnology Information Conserved Domain Database and C-DART tools (Geer et al. 2002; Sayers et al. 2012; Wheeler et al. 2003). To examine evolutionary history, we used the KEGG Gene Cluster tool, which examines whether adjacent genes in the query organism are found adjacent to one another in other organisms in the database, which indicates that the adjacent genes tend to travel together over evolutionary time. We also used the Search Tool for the Retrieval of Interacting Genes/Proteins (STRING) tool (version 9.05), which identifies predicted protein interactions based on the genomic contexts of the genes that encode them, on high throughput experimental data, expression data, and interaction data documented in publication (Szklarczyk et al. 2011).

Cloning of the *ACIAD1960* gene into pET15b

ACIAD1960 (UniProt: Q6FAX7; Punta et al. 2012) was cloned from *A. baylyi* genomic DNA using polymerase chain reaction (PCR). Primers were obtained from Sigma-Genosys. The forward primer sequence is 5′-GAAGGATTTTAGCCATATGGCGATTATCAATAAAGATAAAGC-3′ and contains an *Nde*I restriction site (underlined). The reverse primer sequence contains a *Bam*HI restriction site (underlined) and is 5′-TGCCCCTAAAGGATCCGATAACATAAAATTATCCTTTCCCC-3′. PCR amplification conditions consisted of 10 ng of genomic DNA in the presence of 0.3 μmol/L primers, using KOD Hot Start Master Mix (EMD Millipore, Billerica, Massachusetts, USA). Cycling conditions consisted of an initial polymerase activation step of 95 °C for 2 min, followed by 30 cycles of denaturation of 95 °C for 20 s, annealing at 56 °C for 10 s, elongation at 70 °C for 20 s, with a final elongation of 72 °C for 5 min. The purified PCR product (QIAquick PCR purification kit, Qiagen, Valencia, California) and the pET15b vector (Novagen, Madison, Wisconsin) were digested using *Nde*I and *Bam*HI restriction endonucleases (New England Biolabs, Ipswich, Massachusetts) and dephosphorylated using calf intestinal phosphatase (New England Biolabs). The PCR product and vector were ligated using T4 DNA ligase (New England Biolabs) and transformed into One Shot Top10 cells (Invitrogen, Carlsbad, California) for plasmid isolation. The cells were plated onto LB plates containing 50 μg/mL ampicillin.

Expression of the cysteine protease

To induce expression of the protein, freshly transformed individual colonies in *E. coli* BL21(DE3)pLys cells (Invitrogen) were grown overnight in 2 mL of LB media containing 50 μg/mL ampicillin. To 250 mL of media, 1.25 mL of the overnight culture was added and incubated at 37 °C while shaking at 225 r/min. When the optical density at 600 nm was between 0.4 and 0.6 ODU, isopropyl-β-D-1-thiogalactopyranoside (IPTG) was added to a final concentration of 0.5 mmol/L, and protein expression continued for a further 3 h. Cells were harvested by centrifugation at 9000*g* at 4 °C. Cell pellets were stored at −80 °C until purification.

Protein purification

The pET-15b vector adds a 6× histidine tag to the N terminus of the protein, which facilitates purification over Ni-NTA agarose resin (Qiagen). The cell pellets were thawed on ice, and suspended in 15 mL of lysis buffer (100 mmol/L NaH_2PO_4, 10 mmol/L Tris–Cl, pH 8.0). Cells were lysed by sonication using ten 1 s bursts. Lysate was cleared by centrifugation at 9000*g*, 4 °C for 20 min. Cleared lysate was incubated with 6 mL of Ni–NTA agarose resin at 4 °C for 1 h. Resin was loaded into a chromatography column, excess buffer was eluted, and the column was washed with four 6 mL fractions of lysis buffer. Elution of the protein consisted of four 6 mL washes with buffer A (100 mmol/L NaH_2PO_4, 10 mmol/L Tris–Cl, pH 6.3). Samples were stored on ice to minimize potential autoproteolysis. Additional large molecular mass proteins were removed by a 15 min centrifugation step using Amicon Utracel 50K centrifugal filters (EMD Millipore). After this final purification step, the sample was concentrated using an Amicon Utracel 10K centrifugal filter. Fractions were assessed for purification by SDS–PAGE on 4%–20% gels (BioRad, Hercules, California, USA), and visualized by Coomassie staining. Protein concentration was determined by the BCA Protein Assay (Thermo Fisher Scientific). Additionally, all fractions were assessed by enzyme activity assay to test for the presence of protease activity. Samples were stored at 4 °C, with the addition of leupeptin to a final concentration of 2 mmol/L.

Enzyme activity assay

The esterase activity of the enzyme was determined spectrophotometrically on a Cary 100 UV-Vis spectrophotometer at 405 nm, using *p*-nitrophenyl acetate (pNPA; Sigma-Aldrich) as a substrate. Assay conditions were 12 mmol/L Tris–sulfate (pH 7.6), at room temperature. Samples were equilibrated in appropriate buffer using Amicon Ultra centrifugal 10K filters. At this pH and wavelength the molar extinction coefficient of *p*-nitrophenol, $\varepsilon = 9000$ L/(mol·cm) (Morillas et al. 1999). A 35 mmol/L pNPA stock solution was made in methanol. For an assay, in a 1 mL cuvette, pNPA was added to a final concentration of 0.100 mmol/L in assay buffer. To this, 200 μL of purification fraction was added to initiate the reaction. One unit of esterase activity is defined as the amount of enzyme that hydrolyzes 1 μmol of pNPA per minute. Affinity labeling with bromopyruvic acid was carried out as follows. A 100 mmol/L bromopyruvic acid (Sigma-Aldrich) stock solution was made in deionized water. The assay conditions were as described above, but with the solution in the cuvette brought to a final concentration of 5 mmol/L bromopyruvic acid prior to adding enzyme.

Tellurite resistance

Overnight cultures in LB (with kanamycin for the mutants) incubated at 37 °C with high aeration were used to inoculate broth containing potassium tellurite (K_2TeO_3; Sigma-Aldrich), using 1:1000 dilution. Tubes were incubated with high aeration at 37 °C for 24 h, after which the density of cell growth was measured using optical density at 600 nm (OD_{600}). Cultures with OD_{600} of 1.0 or higher were diluted in sterile saline (10 g/L NaCl) and the OD_{600} of the dilution was used instead to calculate the actual OD_{600} of the densest cultures. Control cultures without tellurite were used to normalize the values to 100%. The nonpolar insertion–deletion mutants in *stiP* and some of the genes that surround it were obtained from the whole-genome collection at Genoscope (de Berardinis et al. 2008). The insertion site was confirmed by PCR.

Population growth dynamics

Cells were grown in Minimal Davis Broth (Sigma-Aldrich) supplemented with 10 mmol/L succinate for 18–24 h at 37 °C with high aeration, supplemented with 10 μg/mL kanamycin for the mutants. Seven-day growth curves were done using 25 mL of this broth in flasks, at 37 °C with high aeration. Colony-forming units per millilitre were determined using 10-fold dilution and plating on LB (wild-type cells) or LB–kanamycin (mutant cells). Yields from cells grown in LB for 18–24 h at 37 °C with high aeration, supplemented with 10 μg/mL kanamycin for the mutants, were determined using 10-fold dilution and plating on LB (wild-type cells) or LB–kanamycin (mutant cells).

Atomic force microscopy (AFM)

Cells were grown in LB for 18–24 h at 37 °C with high aeration, supplemented with 10 μg/mL kanamycin for the mutant. Next they were inoculated 1:25 into fresh broth and incubated for 4 h at 37 °C with high aeration. After 4 h, 1.5 mL of cells was collected by brief microcentrifugation. Cells were washed by resuspending in 1 mL of ice-cold sterile Milli-Q water, then pelleted again, a total of 3 times. After the third resuspension, a dilution series was prepared in ice-cold sterile Milli-Q water. To mount the cells for imaging, 1 cm mica disks (Ted Pella, Redding, California, USA) were attached to an AFM mounting puck using adhesive. We used tape to cleave the mica, resulting in a very smooth surface, and then applied 15 μL of each dilution to the mica. Samples were air-dried at room temperature for at least 24 h before imaging. Mutant and control wild-type cells were prepared in parallel.

Samples were imaged with a Multimode AFM and Nanoscope IIIa controller made by Digital Instruments (now owned by Bruker, Ewing, New Jersey, USA). We used standard silicon cantilevers ($f \approx 300$ kHz) operated in tapping mode, and images were acquired in air at ambient conditions.

The only image postprocessing performed was to planefit AFM images to correct for tilt. To quantify the observed morphology changes, we measured the length and width of a random sampling of cells in multiple images. To randomly choose cells to measure, we assigned a number to every cell in an image, and then used an online number generator to select 100 cells at random (www.random.com, accessed October 2012). Looking at cross-sections of the cell shape, the length or width of a cell was defined as the measured distance between the local minima associated with the ends of the cell for the long or short axis, respectively.

Results

As discussed in the Introduction, as a result of our work on genes active during LTSP, we chose *ACIAD1960*/*stiP* as our gene of interest. Subsequently, our first step was to use bioinformatics to suggest possible properties of this gene to explore further.

Bioinformatics

Predicted domains

We used 2 tools to compare the sequence of StiP with that of other conserved proteins: the National Center for Biotechnology Information (NCBI) Conserved Domain Architecture Retrieval Tool and the Kyoto Enzymes, Genes, and Genomes (KEGG) database. According to both databases, StiP (ACIAD1960; UniProt Q6FAX7) is predicted to be 383 aa in length, with a calculated molecular weight of 42 995 and a calculated pI of 5.96 (Barbe et al. 2004; http://web.expasy.org/cgi-bin/compute_pi/, accessed 7 June 2013; Artimo et al. 2012).

Looking further, we find StiP has various predicted domains, depending on which database is used to call the domains as shown in Fig. 1. As of 7 June 2013, the NCBI Tool identified nearly the entire length of the protein as Domain of Unknown Function (DUF) number 2983 (DUF2983; Geer et al. 2002; Sayers et al. 2012; Wheeler et al. 2003). On the same date, the KEGG database found multiple domains including a phosphoribosyl transferase (PRTase) for the N-terminal 2/3 of the protein, a PELOTA domain for the C-terminal 1/3, and a DUF1796 papain-like cysteine protease domain overlapping these 2 (Hunter et al. 2012; Kanehisa and Goto 2000; Kanehisa et al. 2012).

Fig. 1. Predicted domains in StiP. The KEGG and NCBI databases were used to analyze the amino acid sequence of ACIAD1960. The protein is shown at the top (white fill). It is 383 aa long, and tic marks above the protein indicate every 50 aa. Predicted domains are depicted beneath the protein: DUF1796 probable cysteine protease (diagonal stripes), PRTase (black fill), PELOTA (grey fill). The 4-point star indicates the approximate position of the autocatalytic cleavage site for the protease.

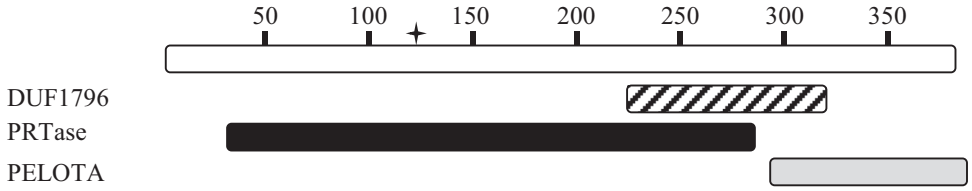

Fig. 2. Genes associated with StiP through proximity, annotation, predicted function, or STRING. The *stiP* gene is filled in black and labeled, and a few other genes are marked with their ACIAD number. Genes *1950*, *1951*, and *1970*, outlined in grey, are neighboring genes included only for context. Predicted operons are marked by solid black lines above the genes (Price et al. 2005). A dotted black line beneath the arrows marks the "TerY-P Triad" (Anantharaman et al. 2012). Proteins predicted to be composed of domains that occur at least twice in this set of related genes are filled to indicate the domains as follows: TerY domain, black dots on white background; TerD domain, black diagonal on white background; 2 consecutive nonoverlapping TerD domains: grey diagonal on white background; TerD,vWA, black diagonal on grey background; TerY-C domain, black dots on grey background; TerC domain, vertical stripes. Table 1 provides more information on the protein annotations.

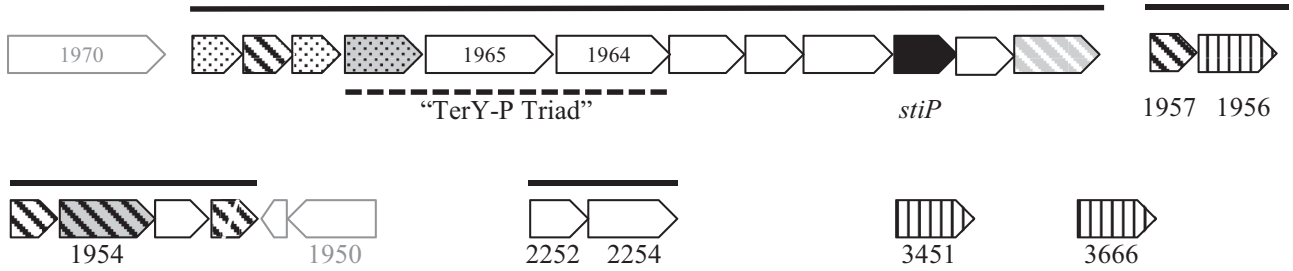

Search tool for the retrieval of interacting genes and proteins (STRING)

In a second bioinformatic inquiry, we used the STRING tool (version 9.05), which identifies predicted protein or genetic interactions based not only on sequences but also on high throughput experimental data, expression data, and interaction data documented in publication (Szklarczyk et al. 2011).

The *stiP* gene is found in a STRING network with 10 genes, all of which are encoded nearby. Note that *A. baylyi* genes are numbered consecutively with the "ACIAD" prefix. The 10 genes are *ACIAD1952*, *ACIAD1953*, *ACIAD1955*, *ACIAD1957*, *ACIAD1958*, *ACIAD1959*, *ACIAD1961*, *ACIAD1962*, *ACIAD1963*, and *ACIAD1968*. STRING networks for these 10 proteins ultimately lead to a larger network that includes all of the genes from *ACIAD1952* to *ACIAD1969* inclusive, and as their similar numbers indicate, they are all encoded in 1 block on the *A. baylyi* chromosome, which we have designated the StiP–Ter cluster. The evidence connecting these proteins includes similar gene order in many organisms ("neighborhood" in the STRING parlance), gene fusion data (in which the gene encoding protein StiP has been fused to one of the other genes in the network, creating a multidomain protein), and co-occurrence in many genomes.

The proteins in the StiP–Ter cluster and their annotations are given in Fig. 2 and detailed in Table 1. Many of these proteins are annotated as *te*llurite *r*esistance proteins, as denoted by "Ter" domains, suggesting StiP may also be required for such resistance. In *A. baylyi*, StiP is encoded in a cluster that encodes proteins with TerD, TerC, and TerY domains (Anantharaman et al. 2012; Barbe et al. 2004). Given the strong association of StiP's STRING network with tellurite resistance, for completeness, we also include in Fig. 2 and in Table 1, *A. baylyi* genes at other loci that contain TerC domains.

Proteins with TerD domains are predicted to assemble into a supramolecular structure that binds to Ca^{2+} or other ions, and that might synthesize a small intracellular messenger (Anantharaman

Table 1. *Acinetobacter baylyi* tellurite-resistance-related proteins.

ACIAD No.	Annotated domains
1969	TerY
1968	TerD
1967	TerY
1966	TerY-C
1965	PP2C_2 phosphatase[a]
1964	STYKIN kinase[a]
1963	ATP-grasp[a]
1962	PRTase_2, TRSP[a]
1961	Haloacid dehalogenase-like hydrolase
1960	StiP; PRTase_1, PELOTA_12/DUF1796[b]
1959	TIM-Barrel C–C_bond_lyase[a]
1958	TerD, TerD[c]
1957	TerD
1956	TerC/DUF475[b] integral membrane protein
1955	TerD
1954	TerD, VWA-TerF-like[b]
1953	AIM24[a]
1952	TerD
2252	TelA[a]
2254	DUF4164[d]
3451	TerC/DUF475[b] integral membrane protein
3666	TerC/DUF475[b] integral membrane protein[e]

Note: Data is from Anantharaman et al. 2012; Kanehisa and Goto 2000; Kanehisa et al. 2012.

[a]Often found in association with other Ter stress proteins.

[b]The solidus (/) in the domain name indicates that the predicted domains overlap.

[c]Protein has 2 adjacent, nonoverlapping TerD domains.

[d]Annotated name is KlaA/KilA.

[e]Amino acids 88–290 of a 326 aa protein.

et al. 2012). Proteins with TerY domains are predicted to assemble into a complex with a kinase and a phosphatase (in *A. baylyi*, ACIAD1965 and ACIAD1964), possibly resulting in synthesis of a small intracellular messenger molecule (Anantharaman et al. 2012). Finally, proteins with TerC domains are predicted to have 7 transmembrane helices and might also have intramembrane metal binding sites (Anantharaman et al. 2012). The inner membrane TerC proteins may form a complex with the TerD domain proteins (Anantharaman et al. 2012).

Taken together, these results suggest that StiP is part of a large group of proteins that carry out a complex function or functions related to detecting and responding to one or more environmental stressors of which tellurite is one.

KEGG gene clustering

KEGG "gene clusters" are groups of spatially contiguous genes that are also spatially contiguous (or nearly so) in other genomes, identified using sequence comparisons of the proteins encoded by each gene. Gene clusters indicate the set of genes has remained physically together over large amounts of time suggesting a common functional role. Furthermore, closely related gene clusters appearing in organisms distantly related to the query genus, but not in close relatives to the query genus, imply that the cluster of genes moved together by way of horizontal (lateral) gene transfer.

The KEGG Gene Cluster Tool finds *stiP* in a cluster that includes all the genes from *ACIAD1955* through *ACIAD1969*. This gene cluster is not found in close relatives of *A. baylyi*. Although the database contains 1 isolate of *Acinetobacter oleivorans*, 1 isolate of *Acinetobacter calcoaceticus*, and 12 isolates of *Acinetobacter baumannii*, the cluster is not found in any of these *Acinetobacter* spp. genomes. In contrast, the 5 most similar gene clusters are only found in distant relatives of *A. baylyi* (degree of relation to *A. baylyi* given in parentheses): (*i*) *Pseudomonas syringae* pv. Tomato DC3000 (same order, *Pseudomonadales*), (*ii*) *Pseudomonas putida* ND6, (*iii*) *Pseudomonas syringae* pv. Phaseolicola 1448A, (*iv*) *Pseudomonas syringae* pv. Syringae B728a, and (*v*) *Burkholderia* sp. strain 383 (same phylum, *Proteobacteria*). That this gene cluster is found not in close *Acinetobacter* relatives but rather only in other genera suggests *A. baylyi* acquired the genes through horizontal gene transfer and the genes probably contribute to a common functional role.

Because genes *ACIAD1952* and *ACIAD1953* were in a STRING with *stiP* but not in the same gene cluster, we queried the KEGG database again and found those 2 genes are in their own gene cluster. The 1952–1953 cluster, like the larger cluster described in the previous paragraph, is not found in any of the *Acinetobacter* genomes in the database but rather is found in distant relatives including (*i*) 3 *Pseudomonas* genomes (same order, *Pseudomonadales*), (*ii*) *Aromatoleum aromaticum* EbN1 (same phylum, *Proteobacteria*), (*iii*) *Thiocystis violascens* (same phylum, *Proteobacteria*), and (*iv*) *Allochromatium vinosum* (same phylum, *Proteobacteria*). These results further substantiate the acquisition of this block of genes by *A. baylyi* through horizontal gene transfer. Using *ACIAD1954* to seed another gene cluster search identifies gene clusters that were also found using StiP or *ACIAD1952* and *ACIAD1953* to perform the search. Overall, the KEGG database identified 147 genomes that contain close StiP homologues, all of which are in the context of a StiP–Ter cluster containing at least 1 protein with a Ter domain. The genomes include very distant relatives, such as species assigned to phyla *Acinetobacteria*, *Firmicutes*, and *Deinococcus–Thermus*.

Bioinformatics summary

Considered as a whole, the bioinformatics analysis suggests that StiP is part of a cluster of proteins that has spread through a variety of bacterial lineages via horizontal gene transfer, and that they probably share a function, which might be adapted to particular, though related, purposes within any given organism. The physiological role of this cluster is predicted to include the ability to survive metal oxyanion and (or) other oxidative stressors, of which tellurite is one. The analysis also suggests that the StiP protein in particular is composed of several domains, which may include a PRTase, a PELOTA domain, or a papain-like cysteine protease domain. With this information to guide us, our next step was to clone the protein and test its activity.

Fig. 3. SDS–PAGE analysis of StiP purification. Samples were run on a 4%–20% SDS–PAGE gel and visualized with Coomassie Blue staining. Lanes: 1, Broad-range molecular mass standards; 2, cell lysate; 3, combined nickel affinity resin elution fractions 1 and 2; 4, combined nickel affinity resin elution fractions 3 and 4; 5, postcentrifugal analysis of sample from lane 3; 6, Postcentrifugal analysis of sample from lane 4. Image was converted to greyscale from a color photo.

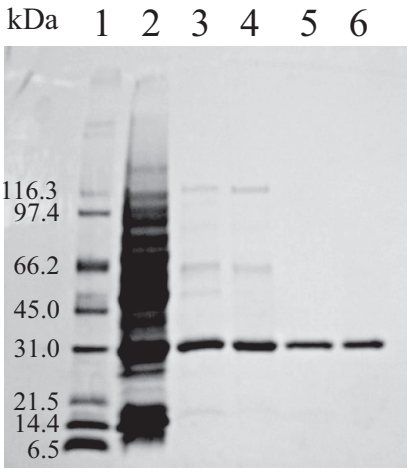

Purification of the *stiP* gene product

The gene encoding StiP was cloned using PCR from *A. baylyi* genomic DNA and inserted into a pET15b vector. This vector adds a 6× histidine tag at the amino terminus of the protein, which facilitates protein purification. Expression in *Escherichia coli* BL21(DE3) cells resulted in soluble protein as demonstrated by comparing the soluble proteins in negative control cells with that of soluble proteins in cells induced to express StiP (data not shown). In Fig. 3, lane 2 shows the SDS–PAGE results for the lysate with a band just beyond the 31.0 kDa mass standard.

To minimize potential degradation of the gene product, we developed a 1 day purification protocol that consists of 2 steps. The first step uses affinity chromatography and takes advantage of the 6× histidine tag on the protein. The protein was bound to the Ni-affinity resin at pH 8.0 and eluted with a buffer at pH 6.3. The results of this purification step are shown in Fig. 3 (lanes 3 and 4), which represent sequential elutions of protein off of the column. In the second purification step, the remaining high molecular mass proteins are removed by a 15 min centrifugal step, using Ultracel 50K centrifugal filters. The final results of the 2-step purification produce a gene product that is greater than 99% homogeneous, as shown in Fig. 3 lanes 5 and 6, which result from sequential elutions shown in lanes 3 and 4, respectively.

The expected size of the ACIAD1960 gene product containing the added sequence of the 6× histidine tag is 45 158 Da. The molecular mass of the purified gene product, based on SDS–PAGE analysis, was estimated to be ~32 400 Da. This result suggests that this protein undergoes an autocatalytic removal of a proregion of ~120 aa (including 20 non-native amino acids from the added 6× histidine tag), and supports the prediction that it is a protease. Given that the band corresponding to the 32.4 kDa product is already present in the cell lysate (Fig. 3, lane 2), it seems that autoprocessing occurs continuously.

Table 2. Purification table for StiP.

Fraction	Total protein (mg)	Total activity (mmol/min)	Specific activity (mmol/(min·mg))	Yield (%)	Purification factor
Cell lysate	51.1	0.292	0.0057	100	1
Ni–NTA resin	5.4	0.173	0.0318	59.3	5.6
Post-centriprep	0.5	0.0492	0.1007	16.8	17.3

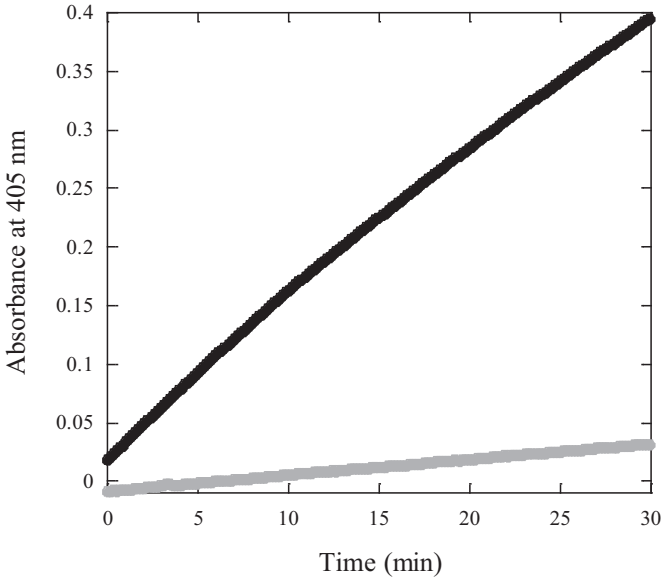

Fig. 4. StiP is a cysteine protease. The esterase activity of purified StiP (6 μmol/L) was monitored at 405 nm, in the absence (black line) and presence (grey line) of a cysteine-specific affinity label (5 mmol/L bromopyruvic acid). The activity decreased from 1.67×10^{-3} to 1.49×10^{-4} units, a reduction of 91%.

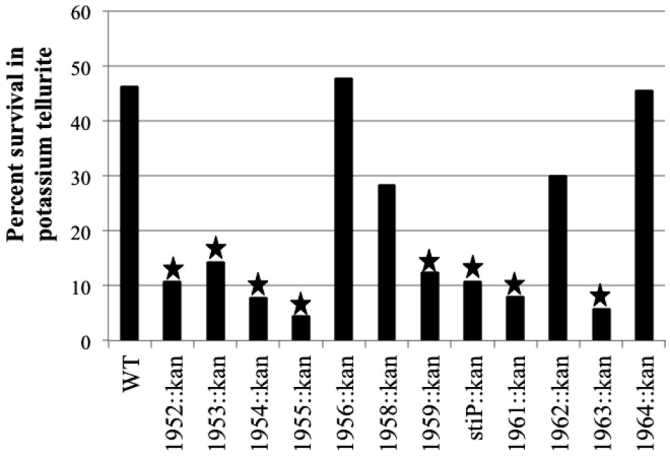

Fig. 5. Mutations in the *stiP–ter* cluster cause hypersensitivity to potassium tellurite. Overnight cultures of cells in Luria–Bertani (with kanamycin in the case of the mutants) were used to inoculate fresh broth containing 6.25 mmol/L potassium tellurite, then their survival rate was measured after 18 h of incubation. *stiP* and many of the genes associated with it show a statistically significant sensitivity to tellurite, as indicated by the stars. WT, wild type.

All papain-like cysteine proteases are synthesized as inactive precursors and undergo proteolytic autoprocessing of an N-terminal proregion to become activated (Kagawa et al. 2000; Mach et al. 1994; Quraishi and Storer 2001; Vernet et al. 1991, 1995; Zinovkin et al. 2003). Further, elution with a buffer of lower pH appears to facilitate autoprocessing, consistent with previous findings that acidic conditions favor this event (Mach et al. 1994; Vernet et al. 1991, 1995).

Taken together, the bioinformatics and the protein purification results imply that this protein is a papain-type cysteine protease because (*i*) this was one of the possible domain types suggested by bioinformatics and (*ii*) cysteine proteases autoprocess a proregion for activation, which is consistent with the smaller size of the purified protein, respective to its predicted gene size. These results suggested we should test the purified protein for cysteine protease activity.

Test of *stiP* for cysteine-specific proteolytic activity

We first assessed whether the gene product had proteolytic activity. We performed esterase activity assays using p-NPA as a substrate. This substrate is commonly used to measure proteolytic activity; cleavage releases the pigmented compound *O*-nitrophenol. Figure 4 and Table 2 give these results. In Fig. 4, the black line shows the p-NPA kinetic profiles for the purified gene product. Based on this activity assay, the results of the 2-step purification are shown in Table 2. Overall, this protocol results in a 17.3-fold increase in purification of the gene product, with an ~17% yield in activity of enzymatic activity.

To further test whether the protein is a cysteine protease, we used 5 mmol/L bromopyruvic acid, an active site cysteine-specific affinity label. Only proteases that have an active site cysteine are inactivated by bromopyruvic acid (Alliel et al. 1982; Kameshita et al. 1979).

As shown by the gray line in Fig. 4, the presence of this compound reduced the activity by 91%, supporting identification of the gene product as a cysteine protease.

Effects of *stiP* deletion on:

Cell growth in the presence of tellurite oxyanion

Having substantiated the prediction that StiP is a cysteine protease, we investigated another bioinformatic prediction, namely that StiP is part of a cluster of proteins with a collective function that includes the ability to survive metal oxyanion and (or) other oxidative stressors, of which tellurite is one.

To test this prediction we grew wild-type *A. baylyi* and *stiP*::*kan-tdk* nonpolar insertion–deletion mutants (de Berardinis et al. 2008) in the presence of potassium tellurite (K_2TeO_3). This gene cassette was designed to be nonpolar and it has been experimentally determined to be non-polar in a whole-genome study in which the cassette was used to determine the essentiality or dispensability of 97% of the 3197 annotated protein-coding genes in *A. baylyi* (de Berardinis et al. 2008). We also tested insertion–deletion mutants missing one of the surrounding genes predicted to share the tellurite resistance function. After 24 h we assessed population growth using optical density. The results showed that deletion of *stiP* or any 1 of 7 of its 11 neighbors led to a statistically significant reduction in cell growth in the presence of tellurite ($p < 0.05$ using a 1-tailed, unpaired, equal variance Student's *t* test) (Fig. 5). This indicates that *stiP* and most of its neighbors are required for normal cell growth in the presence of potassium tellurite. Note that the *ACIAD1958*::*kan-tdk* mutant is not as sensitive to tellurite as the *stiP*::*kan-tdk* and *ACIAD1959*::*kan-tdk* mutants, so that the *kan-tdk* cassette, designed to be nonpolar and shown to be nonpolar in many other contexts (de Berardinis et al. 2008), is likely not

Fig. 6. Long-term cultures of ACIAD *1960*::*kan-tdk* mutants compared with wild type. Minimal succinate broth cultures were inoculated 1:1000 using overnight broths as the inoculum. Colony-forming units (CFU/mL) were determined at 18 h, 2 days, and 7 days postinoculation using serial dilution. The results of 8 independent trials of wild type (□) and mutant (●) are depicted. By day 7, the mutant population is significantly lower than the wild-type population ($p = 0.02$).

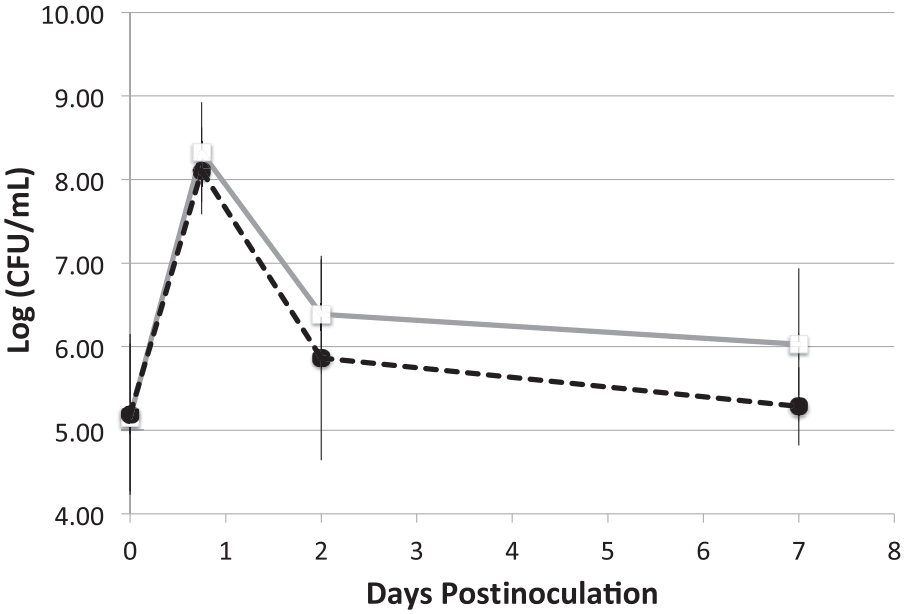

causing the loss of tellurite resistance in the *stiP*::*kan-tdk* mutant due to polar effects.

To test whether tellurite directly affects the activity of StiP, as opposed to having a more indirect effect on StiP via its environment, we characterized StiP's enzymatic activity in the presence of K_2TeO_3 in experiments like those shown in Fig. 4. Specifically, we found no change in activity of StiP in the presence of 1 mmol/L K_2TeO_3 (data not shown), suggesting that TeO_3^{2-} resistance is not directly linked to altered StiP activity under the conditions that we tested. To our knowledge, there are no publications regarding the effects of TeO_3^{2-} ion on cysteine proteases.

The *stiP* gene first came to our attention not because of any functional association with tellurite but because of its high expression during LTSP (Lostroh and Voyles 2010). Because of this expression pattern, we next examined whether inactivation of *stiP* affects population dynamics during long-term batch culture.

Population growth during LTSP

To test the effects of deleting *stiP* on population growth during LTSP, we inoculated wild-type *A. baylyi* and a *stiP*::*kan-tdk* insertion–deletion mutant into flasks of minimal succinate broth and grew them at 37 °C with high aeration. We sampled this broth at 18 h, 2 days, and 7 days postinoculation and used serial dilution to measure the density of cells at these times as shown in Fig. 6. LTSP commences at about 2 days postinoculation, after the cessation of death phase. The data represent 8 independent trials of each strain, and the *stiP*::*kan-tdk* mutant has significantly lower population after 7 days of incubation ($p = 0.02$, Student's t test).

The data presented thus far show that StiP is a cysteine protease and that its absence renders cells sensitive to tellurite and to one or more stressors that occur during death phase and LSTP. Exposure to tellurite may mimic that stress, which could be oxidative damage, including damage to DNA. In bacteria, a response to DNA damage can sometimes cause alterations to cell morphology, so we next turned our attention to imaging mutant cells using AFM.

Cell morphology

To measure cell morphology we imaged wild-type and *stiP*::*kan-tdk* mutant cells by AFM, as shown in Fig. 7. Figure 7*a* shows an image of wild-type *A. baylyi*, and Figs. 7*b* and 7*c* show images of 2 independent samples of the *stiP*::*kan-tdk* mutant. Multiple independent samples of the wild type all looked like Fig. 7*a*, indicating a fairly homogeneous population of cells. In contrast, the mutants display highly variable cell morphology as evident from the disparate appearance of cells in Figs. 7*b* and 7*c*. Figures 7*b* and 7*c* are representative of the kinds of cells observed on multiple independent mutant samples. Table 3 gives mean length, width, and length/width ratios for a random sampling of 100 cells from each of the panels in Fig. 7. The measurements confirm the qualitative observations that the wild-type cells are consistently shorter and wider than the mutant. In addition, the relative homogeneity of the wild type is quantitatively evident in lower standard deviations for its measured values as compared with the mutant.

Table 3. Mean length and width measurements for cell populations in Fig. 7.

	Wild type (Fig. 7*a*)	*stiP*::*kan-tdk* (Fig. 7*b*)	*stiP*::*kan-tdk* (Fig. 7*c*)
Length (μm)	1.4±0.3	1.8±0.5	1.9±0.9
Width (μm)	0.9±0.1	0.8±0.2	0.8±0.1
Length/width (μm)	1.6±0.4	2.4±0.9	2.4±1.2

Note: To better show cell detail, images are 10 μm × 10 μm panels cropped from 30 μm × 30 μm larger images. Measurements here were taken on a random sample of 100 cells/image from the larger images. Given uncertainties are 1 standard deviation from the mean.

Discussion

The results documented in this paper demonstrate that the ACIAD1960 protein, found in *Acinetobacter* and in many other species, should no longer be considered hypothetical. We have named it StiP to reflect its initial experimental description as a LTSP starvation-induced gene and the new discovery, reported here, that it encodes a cysteine protease.

StiP has been predicted to be composed of a variety of domains, of which a cysteine protease was only one. Our results (Fig. 3) show autocatalytic removal of an approximately 12.7 kDa peptide, consistent with the predicted size of proregion sequences of papain-

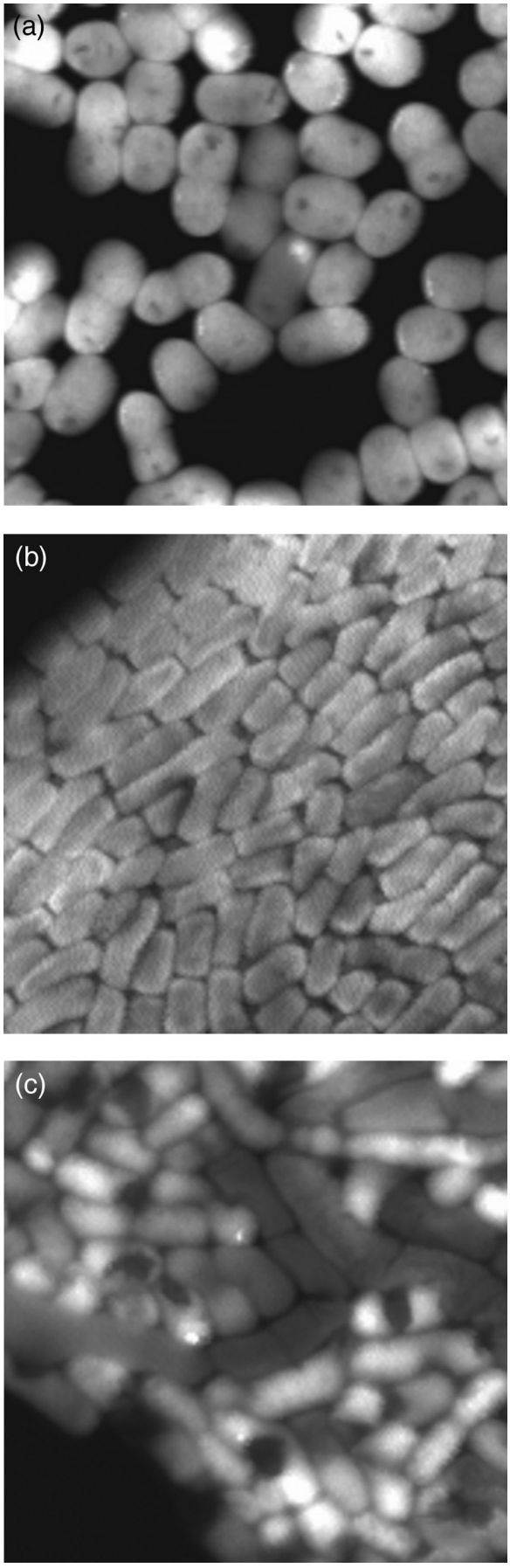

Fig. 7. The *stiP*::*kan-tdk* mutant has altered size and morphology. Atomic force microscopy images of (*a*) wild-type *Acinetobacter baylyi* and (*b*) and (*c*) *stiP*::*kan-tdk* mutant. All images are 10 μm × 10 μm. The wild-type cells are a relatively homogeneous population of coccobacillary cells with mean length/width ratio of 1.6. In contrast the mutant cells display a highly variable cell morphology but are on mean more rod shaped with an mean length/width ratio of 2.4.

like cysteine proteases (Kagawa et al. 2000; Mach et al. 1994; Quraishi and Storer 2001; Vernet et al. 1991, 1995; Zinovkin et al. 2003). This autocatalytic cleavage removes part of the predicted PRTase domain, calling into question whether that domain assignment is correct. Furthermore, the predicted protease domain also overlaps the PELOTA domain, also calling that annotation into question. Among the 2387 bacterial genomes in the KEGG database (accessed 28 July 2013), there are 147 close StiP homologues. While KEGG still predicts them to have a protease domain, following on a 2012 paper (Anantharaman et al. 2012), some other databases have replaced the protease prediction entirely, leaving only the PRTase (IPRO11215) and PELOTA (IPR028157) predictions. Our results suggest that these particular revised predictions, based on sequence comparisons rather than on experimental data, are incorrect.

Additionally, we showed that *stiP* is part of a large cluster of genes likely dedicated to a common function. Mutations in the cluster create hypersensitivity to tellurite oxyanion. In addition, absence of *stiP* creates a mild growth defect in cells during long-term batch culture. Finally, we showed that absence of *stiP* dramatically alters the morphology of the cells.

This group of properties associated with the StiP–Ter cluster may at first appear disparate; however, we postulate that a common thread weaves them together. In overview, the connection we hypothesize is as follows. Both tellurite exposure and LTSP are stressful conditions in which cells likely have oxidative damage to macromolecules, including DNA. LTSP and DNA damage are also both associated with changes in cell morphology. These observations are relevant because *A. baylyi* cells have a unique response to DNA damage and an unusual complement of DNA repair and cell division genes. This unique response occurs in the absence of the LexA and SulA proteins, responsible for changes in the morphology of *E. coli* in response to damaged DNA, and in the absence of the FtsEX proteins, which comprise a septum-associated ABC transporter that is required for cell division in *E. coli* and sporulation in *B. subtilis*, under certain environmental conditions (Garti-Levi et al. 2008; Reddy 2007). *Acinetobacter baylyi* also lacks a clear OxyR homolog; OxyR and SoxR are the 2 redox-sensitive regulators that control the *E. coli* response to oxidative stress (Blanchard et al. 2007; Pomposiello and Demple 2001).

Acinetobacter baylyi lacks homologs of *lexA*, *sulA*, *ftsE*, *ftsX*, and *oxyR*, leaving open the possibility that other genes play their essential roles. We observed that *stiP* is important for *A. baylyi's* ability to withstand stressors such as those encountered in the presence of tellurite and during long-term batch culture. In light of these observations and the well-known connections between stress, DNA damage, cell morphology, and cell division, we hypothesize that StiP and its associated Ter proteins play a role in regulating cell division in the presence of such stressors. In the remainder of this discussion we elaborate on our experimental results in light of this theory.

We consider first the growth defect observed in the presence of tellurite. Tellurite resistance is an unusual phenotype that is difficult to understand because of a lack of tellurite in natural environments (Taylor 1999). Nevertheless, historically tellurite resistance has been a useful property for isolating pathogenic bacteria and has resulted in the discovery of various Ter operons, such as TelA–KlaB, KilA–KlaA, and "Ter" clusters, which are necessary for resistance to tellurite in those pathogens (Anantharaman et al. 2012; Chasteen et al.

2009; Taylor 1999; Taylor et al. 2002; Turner et al. 2001; Whelan et al. 1995). We used the KEGG database and found that in 147 bacterial genomes, StiP homologues are found in the midst of such Ter clusters (Anantharaman et al. 2012). In *A. baylyi* specifically, StiP is surrounded by genes with TerD, TerC, and TerY domains, which in general are predicted to participate in multiprotein complexes (Anantharaman et al. 2012).

Tellurite is toxic because it causes redox stress and oxidative damage (Fuentes et al. 2007; Sandoval et al. 2011; Turner et al. 1999, 2001). Tellurite causes redox stress because it oxidizes cytoplasmic thiol pools, which normally serve as a source of reductant and which maintain the cytoplasm in its normal reduced state (Fuentes et al. 2007; Turner et al. 1999, 2001). Tellurite also causes oxidative damage by inducing the presence of reactive oxygen species, which can independently and directly damage macromolecules such as lipids, proteins with redox-sensitive sulfhydryl groups, and DNA (Perez et al. 2007; Sandoval et al. 2011). While we have not completed physical characterization of StiP and so cannot say whether the protein has any redox-sensitive sulfhydryl groups, we do know that StiP contains 4 cysteines, including one in its active site. Others have found that biosynthesis of cysteine itself is also affected by exposure to tellurite (Chasteen et al. 2009; Fuentes et al. 2007).

The ubiquity of tellurite resistance genes, despite the lack of tellurite in most environments, probably indicates that artificial exposure to tellurite in the laboratory mimics or even exaggerates a stress response that is provoked by normal aerobic metabolism. This contention is supported by work in *Streptomyces coelicolor*, in which Ter domain proteins do not confer resistance to tellurite but are among the most abundant proteins in the cell during normal aerobic growth (Anantharaman et al. 2012; Sanssouci et al. 2011, 2012; Thomas et al. 2012). Pathogens that infect animals are also exposed to reactive oxygen species during their normal colonization of animals, for example when the bacteria are ingested by macrophages. In *Yersinia pestis*, a StiP–Ter cluster is induced during growth inside cultured macrophages (Anantharaman et al. 2012; Ponnusamy et al. 2011).

StiP–Ter clusters are also associated with many other phenotypes in still other organisms, suggesting that these genes have been adapted to purposes other than tellurite resistance and (or) resistance to oxidative stress. For example, in *E. coli*, *ter* genes are needed for resistance to certain bacteriophages, colicins, and cell-envelope-targeting antibiotics (Collins et al. 2010; Taylor 1999; Taylor et al. 2002; Whelan et al. 1995, 1997). Furthermore, DNA damage caused not by reactive oxygen species but by methyl methanesulfonate, mitomycin C, or UV can be counteracted by a *Clostridium ter* cluster cloned on a multicopy plasmid (in *E. coli*) (Anantharaman et al. 2012; Azeddoug and Reysset 1994). Finally, in extremely radiation- and desiccation-resistant *Deinococcus* spp., a StiP–Ter cluster is induced by DNA damage, ionizing radiation, and desiccation (Liu et al. 2003; Makarova et al. 2007; Tanaka et al. 2004).

Ter proteins have also been found to be induced in response to other environmental triggers not necessarily categorized as "stressful", further suggesting that the genes have been adapted for species-specific purposes. For example, in the plant pathogen *Streptomyces scabies*, a TerD-containing protein was expressed in response to a waxy plant molecule called suberin (Langlois et al. 2003). In another streptomycete, *S. coelicolor*, a StiP–Ter cluster is associated with phenotypes that are reminiscent of the *stiP* phenotypes we observe in *A. baylyi*. For example, the cluster is required for normal spore morphology, similar to the *A. baylyi stiP* gene's effects on cellular morphology (Anantharaman et al. 2012; Sanssouci et al. 2011, 2012). Furthermore, these proteins are needed for normal aerobic growth of *S. coelicolor* (Thomas et al. 2012), reminiscent of the requirement for StiP during exponential aerobic growth of *A. baylyi* in general purpose media (when we examined cell morphology in Fig. 7).

Thus, we see that *A. baylyi*, which lacks the typical bacterial DNA damage related LexA–SulA system for regulating the cell cycle in response to DNA damage, appears to use a *stiP–ter* cluster of genes to regulate cell morphology, possibly in response to oxidative damage and (or) alterations to the normal thiol:redox buffering of the cytoplasm. *Acinetobacter baylyi* also lacks FtsE and FtsX, which form a transmembrane complex that is normally part of the septum formation apparatus in most bacteria. The *stiP–ter* cluster of genes in *A. baylyi* putatively encodes several different transmembrane proteins, including a putative transporter that could conceivably substitute for FtsE and FtsX function. Finally, *A. baylyi* lacks an obvious OxyR homologue; in *E. coli* and many other bacteria, OxyR is a redox-sensitive transcription regulator that induces genes needed to survive oxidative stress. It is possible that one or more of the proteins in the StiP–Ter cluster in *A. baylyi* are redox sensitive and play a role in gene regulation.

Drawing all of these strands of evidence together, we therefore hypothesize that the *stiP–ter* cluster of genes in *A. baylyi* contributes to regulating cell morphology in response to DNA damage or in response to oxidative stress or a loss in cytoplasmic thiol:redox buffering capacity. Certainly, other organisms have adapted homologous *stiP–ter* clusters to some as yet unknown purpose in a DNA damage response, as part of a response to aerobic growth (which inevitably causes reactive oxygen species and oxidative damage), or have adapted those clusters for use in regulating or creating spore morphology. There are several possible mechanistic explanations for why the loss of StiP protein, through deletion or through a lack of proper synthesis, folding, or active site formation, could cause alterations to cellular morphology. First, loss of StiP protease activity would result in the abnormal accumulation of uncleaved target proteins. Their cleaved derivatives might be necessary for detecting or responding to cell size or shape. Second, if StiP is part of a multi-Ter protein complex, parts of that complex may not be able to assemble properly in the absence of StiP, or if the proteins normally cleaved by StiP are part of a multi-Ter protein complex, the absence of StiP could indirectly cause a loss of a functional multi-Ter protein complexes.

The discovery of a new group of stress-induced genes important for cell morphology in bacteria that lack the typical SOS response is certainly intriguing and has broad significance. Our work contributes another piece to the puzzle, helping to explain why so-called tellurite resistance proteins are common even though tellurite oxyanions are rare: natural competitive conditions that are mimicked by LTSP are very common in nature, as are oxidative damage and the need to maintain a particular balance of intracellular thiols. The need to regulate cell morphology is similarly ubiquitous. Tellurite resistance genes can apparently be adapted for many essential processes and may be important for cell division in many species. In future work, we will look more closely at how StiP–Ter clusters affect cell morphology under normal and stressful conditions, and we will more thoroughly characterize the biophysical properties of StiP and any Ter proteins with which it interacts.

Acknowledgements

This work was funded by Colorado College Natural Sciences Executive Committee grants to M.A.D., K.M.L., and C.P.L.; by Beland Funds to M.A.D.; and by Colorado College Venture Grants to B.R., S.E.S., and J.A. We wish to thank Andrew Shum and Samuel Zemedkun for developing the protocol to image cells using AFM, the 2012-13 BY101 class and its AFM laboratory mentors Amber Dornbusch, Joshua Kim, and Kaleb Roush, for imaging wild-type and mutant *A. baylyi*.

References

Alliel, P.M., Guiard, B., Ghrir, R., Becam, A.M., and Lederer, F. 1982. Bromopyruvate as an affinity label for Baker's yeast flavocytochrome b_2. Identification of an active-site cysteine and characterization of some cysteine peptides. Eur. J. Biochem. **122**(3): 553–558. doi:10.1111/j.1432-1033.1982.tb06473.x. PMID:7037407.

Anantharaman, V., Iyer, L.M., and Aravind, L. 2012. Ter-dependent stress response systems: novel pathways related to metal sensing, production of a

nucleoside-like metabolite, and DNA-processing. Mol. Biosyst. **8**(12): 3142–3165. doi:10.1039/c2mb25239b. PMID:23044854.

Artimo, P., Jonnalagedda, M., Arnold, K., Baratin, D., Csardi, G., de Castro, E., Duvaud, S., Flegel, V., Fortier, A., Gasteiger, E., Grosdidier, A., Hernandez, C., Ioannidis, V., Kuznetsov, D., Liechti, R., Moretti, S., Mostaguir, K., Redaschi, N., Rossier, G., Xenarios, I., and Stockinger, H. 2012. ExPASy: SIB bioinformatics resource portal. Nucleic Acids Res. **40**(Web Server issue): W597–W603. doi:10.1093/nar/gks400. PMID:22661580.

Azeddoug, H., and Reysset, G. 1994. Cloning and sequencing of a chromosomal fragment from *Clostridium acetobutylicum* strain ABKn8 conferring chemical-damaging agents and UV resistance to *E. coli recA* strains. Curr. Microbiol. **29**(4): 229–235. doi:10.1007/BF01570159. PMID:7765497.

Barbe, V., Vallenet, D., Fonknechten, N., Kreimeyer, A., Oztas, S., Labarre, L., Cruveiller, S., Robert, C., Duprat, S., Wincker, P., Ornston, L.N., Weissenbach, J., Marliere, P., Cohen, G.N., and Medigue, C. 2004. Unique features revealed by the genome sequence of *Acinetobacter* sp. ADP1, a versatile and naturally transformation competent bacterium. Nucleic Acids Res. **32**(19): 5766–5779. doi:10.1093/nar/gkh910. PMID:15514110.

Blanchard, J.L., Wholey, W.Y., Conlon, E.M., and Pomposiello, P.J. 2007. Rapid changes in gene expression dynamics in response to superoxide reveal SoxRS-dependent and independent transcriptional networks. PLoS One, **2**(11): e1186. doi:10.1371/journal.pone.0001186. PMID:18000553.

Chasteen, T.G., Fuentes, D.E., Tantalean, J.C., and Vasquez, C.C. 2009. Tellurite: history, oxidative stress, and molecular mechanisms of resistance. FEMS Microbiol. Rev. **33**(4): 820–832. doi:10.1111/j.1574-6976.2009.00177.x. PMID:19368559.

Collins, B., Joyce, S., Hill, C., Cotter, P.D., and Ross, R.P. 2010. TelA contributes to the innate resistance of *Listeria monocytogenes* to nisin and other cell wall-acting antibiotics. Antimicrob. Agents Chemother. **54**(11): 4658–4663. doi:10.1128/AAC.00290-10. PMID:20713661.

de Berardinis, V., Vallenet, D., Castelli, V., Besnard, M., Pinet, A., Cruaud, C., Samair, S., Lechaplais, C., Gyapay, G., Richez, C., Durot, M., Kreimeyer, A., Le Fevre, F., Schachter, V., Pezo, V., Doring, V., Scarpelli, C., Medigue, C., Cohen, G.N., Marliere, P., Salanoubat, M., and Weissenbach, J. 2008. A complete collection of single-gene deletion mutants of *Acinetobacter* baylyi ADP1. Mol. Syst. Biol. **4**: 174. doi:10.1038/msb.2008.10. PMID:18319726.

Finkel, S.E. 2006. Long-term survival during stationary phase: evolution and the GASP phenotype. Nat. Rev. Microbiol. **4**(2): 113–120. doi:10.1038/nrmicro1340. PMID:16415927.

Finkel, S.E., and Kolter, R. 2001. DNA as a nutrient: novel role for bacterial competence gene homologs. J. Bacteriol. **183**(21): 6288–6293. doi:10.1128/JB.183.21.6288-6293.2001. PMID:11591672.

Fuentes, D.E., Fuentes, E.L., Castro, M.E., Perez, J.M., Araya, M.A., Chasteen, T.G., Pichuantes, S.E., and Vasquez, C.C. 2007. Cysteine metabolism-related genes and bacterial resistance to potassium tellurite. J. Bacteriol. **189**(24): 8953–8960. doi:10.1128/JB.01252-07. PMID:17951385.

Garti-Levi, S., Hazan, R., Kain, J., Fujita, M., and Ben-Yehuda, S. 2008. The FtsEX ABC transporter directs cellular differentiation in *Bacillus subtilis*. Mol. Microbiol. **69**(4): 1018–1028. doi:10.1111/j.1365-2958.2008.06340.x. PMID:18573177.

Geer, L.Y., Domrachev, M., Lipman, D.J., and Bryant, S.H. 2002. CDART: protein homology by domain architecture. Genome Res. **12**(10): 1619–1623. doi:10.1101/gr.278202. PMID:12368255.

Helmus, R.A., Liermann, L.J., Brantley, S.L., and Tien, M. 2012. Growth advantage in stationary-phase (GASP) phenotype in long-term survival strains of *Geobacter sulfurreducens*. FEMS Microbiol. Ecol. **79**(1): 218–228. doi:10.1111/j.1574-6941.2011.01211.x. PMID:22029575.

Hunter, S., Jones, P., Mitchell, A., Apweiler, R., Attwood, T.K., Bateman, A., Bernard, T., Binns, D., Bork, P., Burge, S., de Castro, E., Coggill, P., Corbett, M., Das, U., Daugherty, L., Duquenne, L., Finn, R.D., Fraser, M., Gough, J., Haft, D., Hulo, N., Kahn, D., Kelly, E., Letunic, I., Lonsdale, D., Lopez, R., Madera, M., Maslen, J., McAnulla, C., McDowall, J., McMenamin, C., Mi, H., Mutowo-Muellenet, P., Mulder, N., Natale, D., Orengo, C., Pesseat, S., Punta, M., Quinn, A.F., Rivoire, C., Sangrador-Vegas, A., Selengut, J.D., Sigrist, C.J., Scheremetjew, M., Tate, J., Thimmajanarthanan, M., Thomas, P.D., Wu, C.H., Yeats, C., and Yong, S.Y. 2012. InterPro in 2011: new developments in the family and domain prediction database. Nucleic Acids Res. **40**(Database issue): D306–D312. doi:10.1093/nar/gkr948. PMID:22096229.

Kagawa, T.F., Cooney, J.C., Baker, H.M., McSweeney, S., Liu, M., Gubba, S., Musser, J.M., and Baker, E.N. 2000. Crystal structure of the zymogen form of the group A *Streptococcus* virulence factor SpeB: an integrin-binding cysteine protease. Proc. Natl. Acad. Sci. U.S.A. **97**(5): 2235–2240. doi:10.1073/pnas.040549997. PMID:10681429.

Kameshita, I., Tokushige, M., Izui, K., and Katsuki, H. 1979. Phosphoenolpyruvate carboxylase of *Escherichia coli*. Affinity labeling with bromopyruvate. J. Biochem. **86**(5): 1251–1257. PMID:42643.

Kanehisa, M., and Goto, S. 2000. KEGG: Kyoto Encyclopedia of Genes and Genomes. Nucleic Acids Res. **28**(1): 27–30. doi:10.1093/nar/28.1.27. PMID:10592173.

Kanehisa, M., Goto, S., Sato, Y., Furumichi, M., and Tanabe, M. 2012. KEGG for integration and interpretation of large-scale molecular data sets. Nucleic Acids Res. **40**(Database issue): D109–D114. doi:10.1093/nar/gkr988. PMID:22080510.

Langlois, P., Bourassa, S., Poirier, G.G., and Beaulieu, C. 2003. Identification of *Streptomyces coelicolor* proteins that are differentially expressed in the presence of plant material. Appl. Environ. Microbiol. **69**(4): 1884–1889. doi:10.1128/AEM.69.4.1884-1889.2003. PMID:12676660.

Liu, Y., Zhou, J., Omelchenko, M.V., Beliaev, A.S., Venkateswaran, A., Stair, J., Wu, L., Thompson, D.K., Xu, D., Rogozin, I.B., Gaidamakova, E.K., Zhai, M., Makarova, K.S., Koonin, E.V., and Daly, M.J. 2003. Transcriptome dynamics of *Deinococcus radiodurans* recovering from ionizing radiation. Proc. Natl. Acad. Sci. U.S.A. **100**(7): 4191–4196. doi:10.1073/pnas.0630387100. PMID:12651953.

Lostroh, C.P., and Voyles, B.A. 2010. *Acinetobacter baylyi* starvation-induced genes identified through incubation in long-term stationary phase. Appl. Environ. Microbiol. **76**(14): 4905–4908. doi:10.1128/AEM.01806-09. PMID:20511417.

Mach, L., Mort, J.S., and Glossl, J. 1994. Maturation of human procathepsin B. Proenzyme activation and proteolytic processing of the precursor to the mature proteinase, in vitro, are primarily unimolecular processes. J. Biol. Chem. **269**(17): 13030–13035. PMID:8175723.

Makarova, K.S., Omelchenko, M.V., Gaidamakova, E.K., Matrosova, V.Y., Vasilenko, A., Zhai, M., Lapidus, A., Copeland, A., Kim, E., Land, M., Mavrommatis, K., Pitluck, S., Richardson, P.M., Detter, C., Brettin, T., Saunders, E., Lai, B., Ravel, B., Kemner, K.M., Wolf, Y.I., Sorokin, A., Gerasimova, A.V., Gelfand, M.S., Fredrickson, J.K., Koonin, E.V., and Daly, M.J. 2007. *Deinococcus geothermalis*: the pool of extreme radiation resistance genes shrinks. PLoS One, **2**(9): e955. doi:10.1371/journal.pone.0000955. PMID:17895995.

Morillas, M., Goble, M.L., and Virden, R. 1999. The kinetics of acylation and deacylation of penicillin acylase from *Escherichia coli* ATCC 11105: evidence for lowered pKa values of groups near the catalytic centre. Biochem. J. **338**(1): 235–239. doi:10.1042/0264-6021:3380235. PMID:9931321.

Perez, J.M., Calderon, I.L., Arenas, F.A., Fuentes, D.E., Pradenas, G.A., Fuentes, E.L., Sandoval, J.M., Castro, M.E., Elias, A.O., and Vasquez, C.C. 2007. Bacterial toxicity of potassium tellurite: unveiling an ancient enigma. PLoS One, **2**(2): e211. doi:10.1371/journal.pone.0000211. PMID:17299591.

Pomposiello, P.J., and Demple, B. 2001. Redox-operated genetic switches: the SoxR and OxyR transcription factors. Trends Biotechnol. **19**(3): 109–114. doi:10.1016/S0167-7799(00)01542-0. PMID:11179804.

Ponnusamy, D., Hartson, S.D., and Clinkenbeard, K.D. 2011. Intracellular *Yersinia pestis* expresses general stress response and tellurite resistance proteins in mouse macrophages. Vet. Microbiol. **150**(1–2): 146–151. doi:10.1016/j.vetmic.2010.12.025. PMID:21295415.

Price, M.N., Huang, K.H., Alm, E.J., and Arkin, A.P. 2005. A novel method for accurate operon predictions in all sequenced prokaryotes. Nucleic Acids Res. **33**(3): 880–892. doi:10.1093/nar/gki232. PMID:15701760.

Punta, M., Coggill, P.C., Eberhardt, R.Y., Mistry, J., Tate, J., Boursnell, C., Pang, N., Forslund, K., Ceric, G., Clements, J., Heger, A., Holm, L., Sonnhammer, E.L., Eddy, S.R., Bateman, A., and Finn, R.D. 2012. The Pfam protein families database. Nucleic Acids Res. **40**(Database issue): D290–D301. doi:10.1093/nar/gkr1065. PMID:22127870.

Quraishi, O., and Storer, A.C. 2001. Identification of internal autoproteolytic cleavage sites within the prosegments of recombinant procathepsin B and procathepsin S. Contribution of a plausible unimolecular autoproteolytic event for the processing of zymogens belonging to the papain family. J. Biol. Chem. **276**(11): 8118–8124. doi:10.1074/jbc.M005851200. PMID:11115496.

Reddy, M. 2007. Role of FtsEX in cell division of *Escherichia coli*: viability of *ftsEX* mutants is dependent on functional SufI or high osmotic strength. J. Bacteriol. **189**(1): 98–108. doi:10.1128/JB.01347-06. PMID:17071757.

Sandoval, J.M., Arenas, F.A., and Vasquez, C.C. 2011. Glucose-6-phosphate dehydrogenase protects *Escherichia coli* from tellurite-mediated oxidative stress. PLoS One **6**(9): e25573. doi:10.1371/journal.pone.0025573. PMID:21984934.

Sanssouci, E., Lerat, S., Grondin, G., Shareck, F., and Beaulieu, C. 2011. *tdd8*: a TerD domain-encoding gene involved in *Streptomyces coelicolor* differentiation. Antonie Van Leeuwenhoek, **100**(3): 385–398. doi:10.1007/s10482-011-9593-y. PMID:21638113.

Sanssouci, E., Lerat, S., Daigle, F., Grondin, G., Shareck, F., and Beaulieu, C. 2012. Deletion of TerD-domain-encoding genes: effect on *Streptomyces coelicolor* development. Can. J. Microbiol. **58**(10): 1221–1229. doi:10.1139/w2012-101. PMID:23072443.

Sayers, E.W., Barrett, T., Benson, D.A., Bolton, E., Bryant, S.H., Canese, K., Chetvernin, V., Church, D.M., Dicuccio, M., Federhen, S., Feolo, M., Fingerman, I.M., Geer, L.Y., Helmberg, W., Kapustin, Y., Krasnov, S., Landsman, D., Lipman, D.J., Lu, Z., Madden, T.L., Madej, T., Maglott, D.R., Marchler-Bauer, A., Miller, V., Karsch-Mizrachi, I., Ostell, J., Panchenko, A., Phan, L., Pruitt, K.D., Schuler, G.D., Sequeira, E., Sherry, S.T., Shumway, M., Sirotkin, K., Slotta, D., Souvorov, A., Starchenko, G., Tatusova, T.A., Wagner, L., Wang, Y., Wilbur, W.J., Yaschenko, E., and Ye, J. 2012. Database resources of the National Center for Biotechnology Information. Nucleic Acids Res. **40**(Database issue): D13–D25. doi:10.1093/nar/gkr1184. PMID:22140104.

Szklarczyk, D., Franceschini, A., Kuhn, M., Simonovic, M., Roth, A., Minguez, P., Doerks, T., Stark, M., Muller, J., Bork, P., Jensen, L.J., and von Mering, C. 2011. The STRING database in 2011: functional interaction networks of proteins, globally integrated and scored. Nucleic Acids Res. **39**(Database issue): D561–D568. doi:10.1093/nar/gkq973. PMID:21045058.

Tanaka, M., Earl, A.M., Howell, H.A., Park, M.J., Eisen, J.A., Peterson, S.N., and Battista, J.R. 2004. Analysis of *Deinococcus radiodurans*'s transcriptional response to ionizing radiation and desiccation reveals novel proteins that contribute to extreme radioresistance. Genetics, **168**(1): 21–33. doi:10.1534/genetics.104.029249. PMID:15454524.

Taylor, D.E. 1999. Bacterial tellurite resistance. Trends Microbiol. **7**(3): 111–115. doi:10.1016/S0966-842X(99)01454-7. PMID:10203839.

Taylor, W.H., and Juni, E. 1961*a*. Pathways for biosynthesis of a bacterial capsular polysaccharide. III. Syntheses from radioactive substrates. J. Biol. Chem. **236**: 1231–1234. PMID:13775655.

Taylor, W.H., and Juni, E. 1961*b*. Pathways for biosynthesis of a bacterial capsular polysaccharide. I. Characterization of the organism and polysaccharide. J. Bacteriol. **81**: 688–693. PMID:13775654.

Taylor, D.E., Rooker, M., Keelan, M., Ng, L.K., Martin, I., Perna, N.T., Burland, N.T., and Blattner, F.R. 2002. Genomic variability of O islands encoding tellurite resistance in enterohemorrhagic *Escherichia coli* O157:H7 isolates. J. Bacteriol. **184**(17): 4690–4698. doi:10.1128/JB.184.17.4690-4698.2002. PMID:12169592.

Thomas, L., Hodgson, D.A., Wentzel, A., Nieselt, K., Ellingsen, T.E., Moore, J., Morrissey, E.R., Legaie, R., STREAM Consortium, Wohlleben, W., Rodriguez-Garcia, A., Martin, J.F., Burroughs, N.J., Wellington, E.M., and Smith, M.C. 2012. Metabolic switches and adaptations deduced from the proteomes of *Streptomyces coelicolor* wild type and *phoP* mutant grown in batch culture. Mol. Cell. Proteomics, 11(2): M111.013797. doi:10.1074/mcp.M111.013797. PMID: 22147733.

Turner, R.J., Weiner, J.H., and Taylor, D.E. 1999. Tellurite-mediated thiol oxidation in *Escherichia coli*. Microbiology, **145** (9): 2549–2557. PMID:10517608.

Turner, R.J., Aharonowitz, Y., Weiner, J.H., and Taylor, D.E. 2001. Glutathione is a target in tellurite toxicity and is protected by tellurite resistance determinants in *Escherichia coli*. Can. J. Microbiol. **47**(1): 33–40. doi:10.1139/w00-125. PMID:15049447.

Vernet, T., Khouri, H.E., Laflamme, P., Tessier, D.C., Musil, R., Gour-Salin, B.J., Storer, A.C., and Thomas, D.Y. 1991. Processing of the papain precursor. Purification of the zymogen and characterization of its mechanism of processing. J. Biol. Chem. **266**(32): 21451–21457. PMID:1939177.

Vernet, T., Berti, P.J., de Montigny, C., Musil, R., Tessier, D.C., Menard, R., Magny, M.C., Storer, A.C., and Thomas, D.Y. 1995. Processing of the papain precursor. The ionization state of a conserved amino acid motif within the Pro region participates in the regulation of intramolecular processing. J. Biol. Chem. **270**(18): 10838–10846. PMID:7738022.

Wheeler, D.L., Church, D.M., Federhen, S., Lash, A.E., Madden, T.L., Pontius, J.U., Schuler, G.D., Schriml, L.M., Sequeira, E., Tatusova, T.A., and Wagner, L. 2003. Database resources of the National Center for Biotechnology. Nucleic Acids Res. **31**(1): 28–33. doi:10.1093/nar/gkg033. PMID:12519941.

Whelan, K.F., Colleran, E., and Taylor, D.E. 1995. Phage inhibition, colicin resistance, and tellurite resistance are encoded by a single cluster of genes on the IncHI2 plasmid R478. J. Bacteriol. **177**(17): 5016–5027. PMID:7665479.

Whelan, K.F., Sherburne, R.K., and Taylor, D.E. 1997. Characterization of a region of the IncHI2 plasmid R478 which protects *Escherichia coli* from toxic effects specified by components of the tellurite, phage, and colicin resistance cluster. J. Bacteriol. **179**(1): 63–71. PMID:8981981.

Zambrano, M.M., Siegele, D.A., Almiron, M., Tormo, A., and Kolter, R. 1993. Microbial competition: *Escherichia coli* mutants that take over stationary phase cultures. Science, **259**(5102): 1757–1760. doi:10.1126/science.7681219. PMID:7681219.

Zinovkin, R.A., Erokhina, T.N., Lesemann, D.E., Jelkmann, W., and Agranovsky, A.A. 2003. Processing and subcellular localization of the leader papain-like proteinase of beet yellows closterovirus. J. Gen. Virol. **84**(8): 2265–2270. doi:10.1099/vir.0.19151-0. PMID:12867660.

Zinser, E.R., and Kolter, R. 1999. Mutations enhancing amino acid catabolism confer a growth advantage in stationary phase. J. Bacteriol. **181**(18): 5800–5807. PMID:10482523.

Zinser, E.R., and Kolter, R. 2000. Prolonged stationary-phase incubation selects for *lrp* mutations in *Escherichia coli* K-12. J. Bacteriol. **182**(15): 4361–4365. doi: 10.1128/JB.182.15.4361-4365.2000. PMID:10894750.

Zinser, E.R., and Kolter, R. 2004. *Escherichia coli* evolution during stationary phase. Res. Microbiol. **155**(5): 328–336. doi:10.1016/j.resmic.2004.01.014. PMID:15207864.

Zinser, E.R., Schneider, D., Blot, M., and Kolter, R. 2003. Bacterial evolution through the selective loss of beneficial genes. Trade-offs in expression involving two loci. Genetics, **164**(4): 1271–1277. PMID:12930738.